

# High frequency EPR on dilute solutions of the single molecule magnet Ni<sub>4</sub>

G. de Loubens and A. D. Kent

*Department of Physics, New York University, 4 Washington Place, New York, New York 10003, USA*

V. Krymov and G. J. Gerfen

*Department of Physiology and Biophysics, Albert Einstein College of Medicine, Yeshiva University, 1300 Morris Park Avenue, Bronx, New York 10461, USA*

C. C. Beedle and D. N. Hendrickson

*Department of Chemistry and Biochemistry, University of California San Diego, La Jolla, California 92093-0358, USA*

(Dated: November 10, 2018)

Dilute frozen solutions of the single molecule magnet Ni<sub>4</sub> ( $S = 4$ ) have been studied using high frequency D-band (130 GHz) EPR. Despite the random orientation of the molecules, well defined EPR absorption peaks are observed, due to the strong variation of the splittings between the different spin-states on magnetic field. Temperature dependent studies above 4 K and comparison with simulations enable identification of the spin transitions and determination of the Hamiltonian parameters. The latter are found to be close to those of Ni<sub>4</sub> single crystals. No echo was detected from Ni<sub>4</sub> in pulsed experiments, which sets an upper bound of about 50 ns on the spin coherence time.

Single molecules magnets (SMMs) have been suggested as candidates for qubits in quantum processors<sup>1</sup>. However, the coherence time ( $T_2$ ) of high-spin molecules has not yet been determined. Quantum tunneling of magnetization (QTM) has been widely studied in SMMs<sup>2,3,4</sup>. A recent focus is on coherent QTM in which the tunneling rates may be faster than the rate of decoherence<sup>5,6,7</sup>. Due to inhomogeneous broadening, only a lower bound ( $\approx 0.5$  ns on most of the measured SMMs) of  $T_2$  can be extracted. Furthermore, in SMM crystals the strong dipolar interactions between the molecules (separated by only 1 nm) is expected to drastically reduce the coherence time. In order to determine the latter (*e.g.* through spin echo) and to coherently manipulate the magnetization with microwave pulses in SMMs, it thus may be necessary to work with dilute ensembles of molecules.

SMMs may be diluted in solvents. The drawback of such a method is that the molecules are randomly oriented. However, magnetometry<sup>8</sup> and EPR experiments<sup>9</sup> on randomly oriented powder have been successfully performed. Only recently have dilute frozen solutions been studied by high frequency (HF) techniques. Frequency domain spectroscopy showed that the zero field splitting (ZFS) parameters of Mn<sub>12</sub> clusters diluted in a frozen solvent were almost the same as in the crystal form<sup>10</sup>. Even more interesting, standard microwave pulse experiments have determined a long intrinsic coherence time (few microseconds at  $T = 2$  K) in doped antiferromagnetic wheels (low-spin)<sup>11</sup>.

In this paper we present continuous wave (cw) HF EPR experiments performed on dilute frozen solutions of the SMM Ni<sub>4</sub> ( $S = 4$ ) as a function of temperature between 6 and 30 K. Well defined transitions are observed in the 0–7 Tesla range at  $f = 130$  GHz. Simulations using ZFS parameters close to the ones determined from single crystals<sup>12</sup> and  $D$  and  $g$  strains qualitatively reproduce

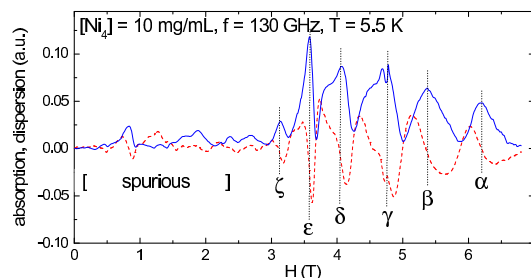


Figure 1: (Color online) EPR spectrum of a 10 mg/mL Ni<sub>4</sub> solution at  $f = 130$  GHz and  $T = 5.5$  K. The dashed and solid lines are respectively the absorption and dispersion channels (a 12 G<sub>pp</sub> field modulation is used). The spurious signal at low field was also observed without Ni<sub>4</sub> molecules in the 1:1 mixture of toluene and dichloromethane.

the spectra measured. No spin echo from the Ni<sub>4</sub> clusters was observed in pulse experiments, which sets an upper limit for  $T_2$  of about 50 ns.

[Ni(hmp)(dmb)Cl]<sub>4</sub>, henceforth referred to as Ni<sub>4</sub>, is a particularly clean SMM with no solvate molecules present in its crystal phase and only 1% (natural abundance) of nuclear spins on the transition metal sites<sup>13,14</sup>. This results in narrower EPR peaks than in many SMMs<sup>12</sup>. The spin Hamiltonian of Ni<sub>4</sub> is to first approximation:

$$\mathcal{H} = DS_z^2 + BS_z^4 + C(S_+^4 + S_-^4) + \mu_B \vec{H} \cdot \hat{g} \cdot \vec{S}, \quad (1)$$

where the first term is the uniaxial anisotropy, the second and third terms are 4<sup>th</sup>-order anisotropy terms, and the last term is the Zeeman energy. The  $S = 4$  ground state of the molecule at low temperature is the consequence of ferromagnetic exchange interactions between the four Ni<sup>II</sup> ( $S = 1$ ) ions. The uniaxial anisotropy leads to a large energy barrier  $|D|S^2 \approx 12$  K to magnetization reversal

between states of projection  $S_z = \pm 4$  along the easy axis of the molecule. The ZFS parameters have been measured on single crystals using HF EPR<sup>12</sup>. In particular, the strong  $C$ -term ( $\approx 10$  MHz) explains the fast tunneling observed at zero field<sup>15</sup>, and a recent analysis shows that the fourth order terms in Eq. 1 may result from a finite ratio of the (second order) single ion anisotropies to exchange constant<sup>16</sup>.

To prepare dilute solutions of  $\text{Ni}_4$ , dried crystals were dissolved in a 1:1 mixture of toluene and dichloromethane. This glass was chosen due to solubility restraints. <sup>1</sup>HNMR spectra were collected for  $[\text{Ni}(\text{hmp})(\text{dmb})\text{Cl}]_4$  and the analogous complexes  $[\text{Ni}(\text{hmp})(\text{CH}_3\text{OH})\text{Cl}]_4$  and  $[\text{Ni}(\text{hmp})(\text{CD}_3\text{OD})\text{Cl}]_4$ , as well as the free ligand 2-hydroxymethylpyridine (hmpH). The proton signals for the bound hmp<sup>-</sup> ligand were positively identified through comparison of the  $[\text{Ni}(\text{hmp})(\text{CH}_3\text{OH})\text{Cl}]_4$  and deuterated  $[\text{Ni}(\text{hmp})(\text{CD}_3\text{OD})\text{Cl}]_4$  complexes. Comparison of the  $[\text{Ni}(\text{hmp})(\text{dmb})\text{Cl}]_4$  and free hmpH spectra confirmed that no free ligand is present, and thus, the  $[\text{Ni}(\text{hmp})(\text{dmb})\text{Cl}]_4$  complex is intact in solution. Most of our EPR experiments were carried out on a 10 mg/mL solution, corresponding to an average distance of 6 nm between molecules.

D-band (130 GHz) EPR spectra were acquired on a spectrometer capable of working in cw and pulse modes. The quadrature detection microwave bridge was designed and built by HF EPR Instruments, Inc. (V. Krymov, New York). During the acquisition in cw mode, a field modulation of 12  $G_{\text{pp}}$  is generated at 100 kHz by a coil surrounding the cavity, and the dispersion and absorption channels<sup>17</sup> are recorded as a function of the external field, generated by a 7 T superconducting magnet. Fig. 1 shows the result of such an experiment performed at 5.5 K on a 10 mg/mL  $\text{Ni}_4$  solution contained in a quartz capillary tube (active volume 0.2  $\mu\text{L}$ ). Large absorption peaks (labeled  $\alpha$  to  $\zeta$  with decreasing field) can be observed above 2.5 T. They are attributed to transitions between spin-states of the dissolved  $\text{Ni}_4$  molecules. The narrow signal around 4.6 T ( $g \approx 2$ ) and the spurious absorption at low field were also measured without  $\text{Ni}_4$  clusters in the solvent, in contrast to the high field peaks. These do not affect the high field part of the spectrum, and we will not discuss them further.

To address the origin of the transitions observed in Fig. 1, we discuss the dependence of the EPR signal on temperature and the comparison with simulations, shown in Fig. 2a and b respectively. The latter were performed using the EasySpin toolbox<sup>18</sup>, which allows calculation of EPR spectra<sup>19</sup> and provides the visualisation tools used in Fig. 3.  $2^\circ \times 2^\circ$  cells in one octant of the upper hemisphere were used to perform the powder average. First, we used the ZFS parameters of  $\text{Ni}_4$  single crystal ( $D = -0.748(5)$  K,  $B = -6 \times 10^{-3}$  K,  $C = \pm 2.9 \times 10^{-4}$  K,  $g_x = g_y = 2.23$ ,  $g_z = 2.3$ )<sup>12,15</sup>, and a convolution by a gaussian of width 0.1 T (dashed curve on Fig. 2b at 6 K). The position of the high field peaks are slightly offset with

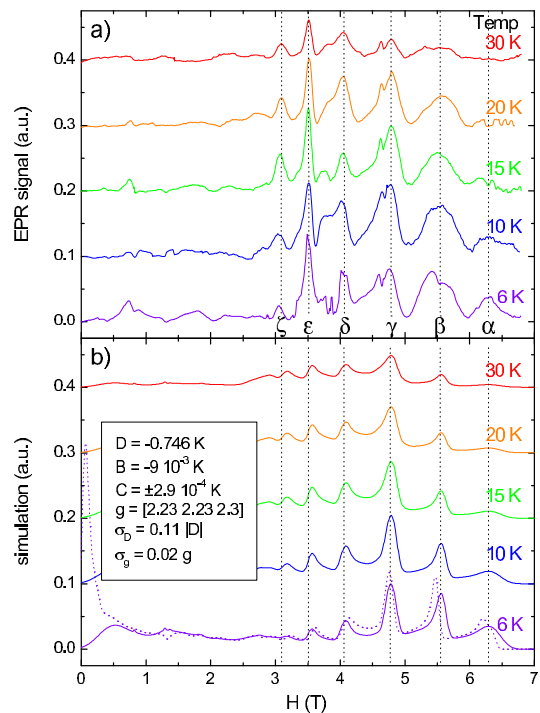


Figure 2: (Color online) a) EPR signal versus temperature. b) The dashed curve is the simulation at 6 K using the ZFS parameters of the single crystal (see text) and a 0.1 T gaussian broadening. The continuous curves have been calculated using the parameters indicated in the inset, that include  $D$  and  $g$  strains.

respect to the data, and a large absorption peak close to zero field is calculated, but not detected.

To improve the position of the calculated peaks, we used slightly different  $D$  and  $B$  parameters ( $D = -0.746(5)$  K,  $B = -9 \times 10^{-3}$  K), and introduced  $D$  and  $g$  strains ( $\sigma_D = 0.11|D|$  and  $\sigma_{\hat{g}} = 0.02\hat{g}$ ), which wash out the low field transitions and lead to an overall better fit to the spectrum. It is known that  $D$  and  $g$  strains influence the lineshapes in SMM single crystals<sup>20</sup>. Random dipolar fields, also expected to play a role, should be less important in dilute solutions due to the larger average distance between neighboring molecules. The simulations reproduce rather well the dependence of the experimental data on temperature. In particular, it can be seen that, on top of the global decrease of the absorption, the simulations reproduce the extinction of the peaks  $\alpha$  and  $\beta$  as the temperature increases. This is expected from Boltzmann statistics, since the difference in population between the lowest energy levels decreases exponentially with temperature (note that  $f = 130$  GHz corresponds to  $T = 6.2$  K). Therefore,  $\alpha$  is associated with a transition from the ground state to the first excited state. However, we were unable to reproduce the lineshapes and the very intense  $\epsilon$  peak. We explored the possibility of having two  $\text{Ni}_4$  species (dissolved and precipitated<sup>10</sup>) in the solution without success. We believe that our dilute solutions are free of precipitate, and it was checked after

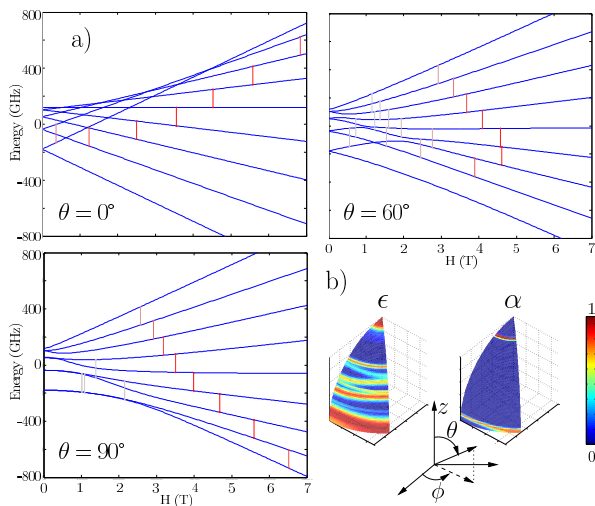


Figure 3: (Color online) a) Energy levels for 3 different angles between the applied field and the molecular easy axis. The transitions corresponding to  $f = 130$  GHz are shown. The stronger the red color, the larger the matrix element of the transition. b) Orientations contributing to transitions  $\alpha$  and  $\epsilon$  (cf. Fig. 1 and 2). Note that in a) and b), all allowed transitions are displayed without regard to the temperature.

each experimental run that the dilute solution contained in the quartz tube was still clear. Increase of the  $D$  and  $g$  strains does not improve the fit either. The values used in the simulations are already larger than the ones fitted on single crystals<sup>20</sup> by a factor 2 to 10. This probably results from the variation in the molecular environment of the SMM clusters in the frozen solution. It is known, *e.g.* in  $\text{Mn}_{12}$  crystals, that this environment plays a critical role<sup>21</sup>. In solution, the strain could also depart from axially symmetric.  $E$ -strain can not be excluded, as simulations performed with  $\sigma_E = 0.05$  K slightly broaden peaks  $\alpha$  to  $\gamma$ .

To better understand the nature of the transitions involved in the EPR spectrum, Fig. 3a shows the energy levels as a function of the angle  $\theta$  between the easy axis of the molecules and the magnetic field (the angle  $\phi$  in the hard plane is set to  $0^\circ$ ). The well-known diagram is obtained for  $\theta = 0^\circ$ , with the low lying transitions at low field. In our experimental case, the ground state transition ( $m = -4 \rightarrow -3$ ) at low field is not observed because the ZFS of  $\text{Ni}_4$  is about 140 GHz, slightly larger than our working frequency. When  $\theta = 90^\circ$ , the ground state transition is on the contrary at the highest field ( $\alpha$  in Fig. 1 and 2). For an intermediate angle, the transitions can also be determined by a full diagonalization of the Hamiltonian (Eq. 1). As a result of the rapid variation of the splittings with the amplitude and the direction of the applied field, certain subpopulations of

molecules are selected, and well defined absorption peaks are observed. Fig. 3b, which shows the orientations contributing to peaks  $\alpha$  and  $\epsilon$ , validates this picture. The influence of the  $C$ -term can be seen for the peak  $\alpha$  (variation between  $\phi = 0^\circ$  and  $\phi = 45^\circ$ ), for which the easy axis of the contributing molecules almost lie in the plane  $\theta = 90^\circ$  (the band near  $\theta = 0^\circ$  is a highly excited transition which does not contribute at low temperature).

Finally, echo experiments ( $\pi/2 - \tau - \pi - \tau$ -echo high power pulse sequences) were conducted at 5.5 K on several dilutions of  $\text{Ni}_4$  (down to 0.5 mg/mL) and on the pure solvent. We did not observe any echo from the  $\text{Ni}_4$  molecules. Let us briefly discuss this result. First, the sensitivity of the experimental setup is sufficient to detect echoes with  $T_2 > 50$  ns in 200 G broad lines from micromolar solutions (*i.e.*  $10^{11}$  spins) of  $S = 1/2$  compounds. Despite the random orientation of the  $\text{Ni}_4$  molecules and the broad absorption lines ( $\approx 2$  to 4 kG), the cw EPR data shows that a small ( $\approx 5\%$ ) but non negligible fraction of the molecules contribute to the signal. Taking into account these factors, it is found that there are still about 30 times more spins than needed to detect an echo if  $T_2 > 50$  ns for the 10 mg/mL  $\text{Ni}_4$  solution. Second, the random orientation makes the intermolecular interaction weak because the effective dilution of the molecules addressed by the microwaves is large. Third, the coupling to nuclear spins can yield coherence times larger than 50 ns<sup>11</sup>. It is not clear whether the coherence time of spin-states oscillations between excited levels (as  $\beta$  to  $\zeta$ ) could be much shorter than the one between the ground state and the first excited states (as  $\alpha$ ). However, an estimation of the spin-lattice relaxation time from direct spin-phonon process<sup>22</sup> using a reasonable value for the transverse speed of sound in the frozen solvent (1000 m/s) yields  $T_1 = 40$  ns at  $f = 130$  GHz and 5.5 K (it increases by a factor 2 at 0 K). This upper bound for  $T_2$  could explain the absence of echo from  $\text{Ni}_4$  in our experiments. It is interesting to note that  $T_1$  is a strong function of frequency ( $\sim 1/f^3$ ). For instance, at 10 GHz and 1.5 K we estimate  $T_1 = 60 \mu\text{s}$ .

In conclusion, we have studied dilute frozen solutions of the SMM  $\text{Ni}_4$  by HF EPR. The clusters have been found to be stable in solution. Despite the random orientation of the anisotropy axes, it is possible to measure EPR spectra with well defined transitions and to deduce that the ZFS parameters of the dissolved molecules are close to the ones in the crystal phase. Thus, the behavior of an isolated  $\text{Ni}_4$  cluster is essentially the same as that of a single crystal.

This work was supported by NSF-NIRT Grant No. DMR-0506946 (ADK) and by NIH Grant No. GM075920 (GJG).

<sup>1</sup> M. N. Leuenberger and D. Loss, Nature **410**, 789 (2001).

<sup>2</sup> J. R. Friedman, M. P. Sarachik, J. Tejada, and R. Ziolo,

- Phys. Rev. Lett. **76**, 3830 (1996).
- <sup>3</sup> L. Thomas, F. Lioni, R. Ballou, D. Gatteschi, R. Sessoli, and B. Barbara, *Nature* **383**, 145 (1996).
  - <sup>4</sup> W. Wernsdorfer and R. Sessoli, *Science* **284**, 133 (1999).
  - <sup>5</sup> S. Hill, R. S. Edwards, N. Aliaga-Alcalde, and G. Christou, *Science* **302**, 1015 (2003).
  - <sup>6</sup> E. del Barco, A. D. Kent, E. C. Yang, and D. N. Hendrickson, *Phys. Rev. Lett.* **93**, 157202 (2004).
  - <sup>7</sup> G. de Loubens, G. D. Chaves-O'Flynn, A. D. Kent, C. Ramsey, E. del Barco, C. Beedle, and D. N. Hendrickson, *J. Appl. Phys.* **101**, 09E104 (2007).
  - <sup>8</sup> M. A. Novak, R. Sessoli, A. Caneschi, and D. Gatteschi, *J. Magn. Magn. Mat.* **146**, 211 (1995).
  - <sup>9</sup> A. L. Barra, D. Gatteschi, and R. Sessoli, *Phys. Rev. B* **56**, 8192 (1997).
  - <sup>10</sup> F. E. Hallak, J. van Slageren, J. Gomez-Segura, D. Ruiz-Molina, and M. Dressel, *Phys. Rev. B* **75**, 104403 (2007).
  - <sup>11</sup> A. Ardavan, O. Rival, J. J. L. Morton, S. J. Blundell, A. M. Tyryshkin, G. A. Timco, and R. E. P. Winpenny, *Phys. Rev. Lett.* **98**, 057201 (2007).
  - <sup>12</sup> R. S. Edwards, S. Maccagnano, E.-C. Yang, S. Hill, W. Wernsdorfer, D. Hendrickson, and G. Christou, *J. Appl. Phys.* **93**, 7807 (2003).
  - <sup>13</sup> E.-C. Yang, W. Wernsdorfer, S. Hill, R. S. Edwards, M. Nakano, S. Maccagnano, L. N. Zakharov, A. L. Rheingold, G. Christou, and D. N. Hendrickson, *Polyhedron* **22**, 1727 (2003).
  - <sup>14</sup> E.-C. Yang, W. Wernsdorfer, L. N. Zakharov, Y. Karaki, A. Yamaguchi, R. M. Isidro, G.-D. Lu, S. A. Wilson, A. L. Rheingold, H. Ishimoto, et al., *Inorg. Chem.* **45**, 529 (2006).
  - <sup>15</sup> C. Kirman, J. Lawrence, S. Hill, E.-C. Yang, and D. N. Hendrickson, *J. Appl. Phys.* **97**, 10M501 (2005).
  - <sup>16</sup> A. Wilson, J. Lawrence, E.-C. Yang, M. Nakano, D. N. Hendrickson, and S. Hill, *Phys. Rev. B* **74**, 140403 (2006).
  - <sup>17</sup> V. Krymov and G. J. Gerfen, *J. Magn. Res.* **162**, 466 (2003).
  - <sup>18</sup> URL <http://www.easyspin.ethz.ch/>.
  - <sup>19</sup> S. Stoll and A. Schweiger, *J. Magn. Res.* **178**, 42 (2006).
  - <sup>20</sup> S. Hill, S. Maccagnano, K. Park, R. M. Achey, J. M. North, and N. S. Dalal, *Phys. Rev. B* **65**, 224410 (2002).
  - <sup>21</sup> E. del Barco, A. D. Kent, S. Hill, J. M. North, N. S. Dalal, E. M. Rumberger, D. N. Hendrickson, N. Chakov, and G. Christou, *J. Low Temp. Phys.* **140**, 119 (2005).
  - <sup>22</sup> E. M. Chudnovsky, D. A. Garanin, and R. Schilling, *Phys. Rev. B* **72**, 094426 (2005).